

Staff, R. A. and Liu, R. (2021) Radiocarbon calibration: the next generation. *Science China Earth Sciences*, 64(3), pp. 507-510.
(doi: [10.1007/s11430-020-9722-x](https://doi.org/10.1007/s11430-020-9722-x))

There may be differences between this version and the published version.
You are advised to consult the publisher's version if you wish to cite from it.

<http://eprints.gla.ac.uk/233783/>

Deposited on 9 February 2021

Enlighten – Research publications by members of the University of Glasgow
<http://eprints.gla.ac.uk>

Title: Radiocarbon Calibration: the Next Generation

Author affiliations:

Richard A Staff^a & Ruiliang Liu^b

^a Scottish Universities Environmental Research Centre (SUERC), University of Glasgow, Rankine Avenue, Scottish Enterprise Technology Park, East Kilbride G75 0QF, UK.

^b School of Archaeology, University of Oxford, 1 South Parks Road, Oxford OX1 3TG, UK.

E-mail: richard.staff@glasgow.ac.uk (R A Staff) or ruiliang.liu@arch.ox.ac.uk (R Liu)

Abstract:

Radiocarbon (^{14}C) dating is the most commonly applied scientific dating methodology for materials spanning the last *circa* 50 to 60 thousand years. However, in order to derive meaningful ages from “raw” analytical measurements, a calibration stage is required whereby samples’ measured ^{14}C determinations are compared with those of empirically derived calibration curves that consist of thousands of ^{14}C measurements of “known age”. These consensus “IntCal” calibration curves are endorsed by the international radiocarbon community, and have recently (August 2020) been updated to include a wealth of new information. In the present Research Highlights article, we first introduce the need for calibration of radiocarbon data, before summarising the advances that have been made to the IntCal curves since their last iterations (published in 2013). Finally, we discuss the chronological implications of the updated calibration curves for the broad radiocarbon dating user community, which includes palaeoenvironmental scientists, geologists, geomorphologists, and palaeoceanographers, as well as archaeologists.

摘要 (abstract) :

对于距今5-6万年内的样品而言，碳十四是目前应用最为广泛的科技测年手段。但是，如若期望从碳十四原始测量值中获取有意义的年代数据，就必须通过校正这一过程，即是将样品的碳十四测量值与由上千组已知年代的碳十四样品所组成的校正曲线进行拟合比对。这些碳十四校正曲线由国际碳十四协会发布，最近一次发布（2020年8月）包含了大量最新研究进展。本文首先介绍了碳十四数据校正的必要性，之后归纳了最新校正曲线较之前代（发表于2013年）所取得的进步，最后，我们总结了最新校正曲线对于包括古环境、地质、地貌形态、古代海洋学以及考古学在内的整个碳十四测年使用团体的重要意义。

Text:

The discovery of the radiocarbon (^{14}C) dating technique in the mid-twentieth century by Willard Libby and colleagues (Libby *et al.*, 1949) revolutionised such fields as archaeology and palaeoclimatology that require robust chronological information to inform their study. Any sample yielding sufficient quantities of carbon could be dated in this manner, with the older age limit of the method (currently *circa* 50 to 60 thousand years ago) having been pushed back significantly since its inception.

However, it soon became apparent that a calibration stage was required in the process to convert “raw” radiocarbon determinations obtained from samples into a meaningful representation of the passing of “real” calendar time (de Vries, 1958). Such calibration is necessary since the concentration of the radioisotope ^{14}C in the ambient atmosphere relative to stable ^{12}C and ^{13}C is not constant through time. This is the result of both variability in the production rate of ^{14}C in Earth’s upper atmosphere – in turn the result of fluctuations in both the geomagnetic field intensity, as well as the strength of the solar wind – and rearrangements in the relative distribution of carbon between the respective reservoirs of Earth’s carbon cycle system.

Calibration is achieved through the comparison of samples’ measured ^{14}C determinations with those of an empirically derived calibration curve that consists of thousands of ^{14}C measurements of “known age” (i.e., independently geochronologically dated) samples. In order to maintain consistency of the method, the international radiocarbon community endorses a set of “definitive” consensus calibration curves that users of the ^{14}C dating method are expected to implement.

Since 2004, compilation of these calibration curves has been overseen by the “IntCal” (International Calibration) Working Group, which release updates at semi-regular intervals as new contributing data become available and knowledge of the Earth system improves. In August 2020, the latest iterations of the consensus calibration curves were published in the journal *Radiocarbon*, superseding the previous “IntCal13” iterations, namely: (i) “IntCal20”, for calibration of ^{14}C samples drawing their carbon from the Northern Hemisphere atmosphere (Reimer *et al.*, 2020); (ii) “SHCal20”, for samples drawing their carbon from the Southern Hemisphere atmosphere (Hogg *et al.*, 2020); and (iii) “Marine20”, for samples drawing their carbon from the ocean surface layer (Heaton *et al.* 2020b).

These new calibration curves have been updated to incorporate a plethora of new data that has been produced by a multitude of scientists, from numerous contributing laboratories over the intervening seven years, with strict data quality criteria needing to be met in order for their inclusion (Reimer *et al.*, 2013a). The statistical methods applied in the generation of the calibration curves from their constituent datasets have also been significantly updated, with a Bayesian spline approach replacing the previous random walk model (Heaton *et al.*, 2020a). All three curves now extend back to 55,000 calibrated years Before Present (cal BP), representing a 5,000 year extension compared to the previous chronological limit.

For the most recent 12,310 calibrated years, the principal curve, IntCal20, consists entirely of ^{14}C measurements of robustly, independently dendrochronologically dated tree-rings, with an extended period back to circa 13,910 cal BP composed of “floating” tree-ring sequences (i.e., those lacking an “absolute” dendrochronology). A significant advancement for IntCal20 is the inclusion of a large number of ^{14}C measurements from individual tree-rings, for the first time providing annual chronological resolution for sections of the curve. To a large extent, this development has been driven by the search for so-called “Miyake events” – very rapid (sub-annual) increases in atmospheric ^{14}C concentration – following the initial discovery by Miyake *et al.* (2012) of one such prominent event that occurred in 774-775 CE (1175-1176 cal BP) and which is attributed to an extreme solar proton event.

Further back in time, the central contributing dataset and key addition to this latest update to the calibration curve is that provided by the Hulu Cave (China) speleothems (Cheng *et al.*, 2018), which are precisely, independently uranium-thorium (U-Th) dated. This dataset is supplemented by data from further floating tree-ring sequences, other speleothems, foraminifera from marine sediment cores, and marine corals. In addition, perhaps the most important supporting data through this older time period remain ^{14}C measurements of plant macrofossil samples picked from the annually laminated (varved) lacustrine sediment cores from Lake Suigetsu, Japan (Bronk Ramsey *et al.*, 2020) which, along with the tree-rings, provide a direct record of atmospheric ^{14}C concentration. This is not the case with the speleothem or marine archives which do not draw their carbon directly from the ambient atmosphere, and consequently require “dead carbon fraction” (DCF) or “marine reservoir” corrections which incorporate additional uncertainties into their ^{14}C determinations.

Users of the radiocarbon dating technique will be most concerned with where differences lie between the new IntCal20 calibration curve (Reimer *et al.*, 2020) and the previous iteration, IntCal13 (Reimer *et al.*, 2013b). As a first order observation, these changes can be summarised as being far more subtle through the Holocene (i.e., the most recent ~11,700 years), for which the calibration curve was already composed of robust, independently dendrochronologically dated tree-rings, whereas more marked modifications are evident further back in time, where the constituent records underlying the calibration curve are less secure.

One brief Late Holocene period of divergence occurs *circa* 50-250 CE (1900-1700 cal BP; Fig.1), where the previous calibration curve has been supplemented with new measurements upon Japanese tree-rings. This time period roughly coincides with the latter half of the Han Dynasty in China, and is historically significant for the arrival of Buddhism into the country. A radiocarbon sample with a measured radiocarbon “age” of 1900 ± 25 ^{14}C yrs BP would now date approximately 50 calibrated years younger using the revised IntCal20 curve compared with the previous IntCal13 curve (Fig.1).

The remainder of the Holocene section demonstrates very similar structure between the IntCal13 and IntCal20 curves (Fig.2a and b). Accordingly, this means that in the field of Chinese archaeology, where the majority of radiocarbon dates are attributed to the Neolithic and Bronze Age, the current

chronological framework remains largely unchanged; the findings of major research programmes involving chronological reconstruction, such as investigating the peopling of the Tibetan Plateau (Chen *et al.*, 2015), the human-land relationship along the Silk Road (Dong *et al.*, 2020), or the emergence of complex society in China (Renfrew and Liu, 2012), would not be significantly affected by the update to the calibration curve.

There is more marked deviation between the IntCal13 and IntCal20 curves in the latest pre-Holocene period (*circa* 14,000 to 12,000 cal BP), however, with much greater detail shown in the updated dataset (Fig.2c), which is largely a result of the addition of a large amount of single year tree-ring data through this interval.

Back further in time, the updated calibration curve largely tracks the previous iteration, albeit that the IntCal20 curve now includes more detailed structure compared to the overly smooth IntCal13. This is the result of the incorporation of new, high resolution data (principally from the Hulu Cave speleothems), as well as the improved statistical methods for synthesising the multiple contributing datasets (Heaton *et al.* 2020a). However, before 33,000 cal BP, there is greater divergence between the previous and updated calibration curves (Fig.2d); between *circa* 42,000 and 33,000 cal BP IntCal20 provides older calibrated ages than IntCal13 (by up to approximately 700 calibrated years *circa* 39,000 cal BP), whereas for the oldest period of time, IntCal20 now provides slightly younger ages (by up to about 1,000 calibrated years *circa* 49,000 cal BP). Again, these revisions are largely the result of the incorporation of the Hulu Cave speleothem data, with their robust underlying U-Th timescale.

Atmospheric ^{14}C concentration in the Southern Hemisphere is slightly depleted relative to the Northern Hemisphere, which is related to the greater surface area of ocean in the former and the related air-sea $^{14}\text{CO}_2$ flux. Consequently, ^{14}C calibration in the Southern Hemisphere requires a separate curve, SHCal20 (Hogg *et al.*, 2020), which, like its Northern Hemisphere counterpart, has been updated with the implementation of the improved statistical integration approach as well as the addition of new tree-ring data. Nevertheless, a curve composed solely of Southern Hemisphere data is only possible for short time intervals (*circa* 2140 to 0 cal BP, 3520 to 3453 cal BP, 3608 to 3590 cal BP, and 13,140 to 11,375 cal BP), and therefore Northern Hemisphere data from IntCal20 need to be utilised for the remainder of SHCal20, applying a statistical model to account for the variable inter-hemispheric offset in atmospheric ^{14}C concentration. From the period for which contemporaneous data are available from the Northern and Southern Hemispheres, a time-varying offset averaging 36 ± 27 ^{14}C years is demonstrated (with the Southern Hemisphere apparently older).

For regions within the intertropical convergence zone (ITCZ), it is recommended to use a mixed curve to account for the influence of both Northern and Southern Hemisphere air masses within these tropical and sub-tropical regions (Hogg *et al.*, 2020).

Finally, Marine20 applies to samples from the conceptual globally-averaged mixed ocean layer (Heaton *et al.*, 2020b), which is depleted in ^{14}C relative to the atmosphere, and which smooths out higher frequency signal, due to the residence time of carbon in the ocean. This depletion is temporally

and spatially variable, and therefore region-specific marine radiocarbon reservoir age corrections must be additionally applied. The curve is specifically for samples from non-polar regions (defined approximately as 40°S to 40°N (Pacific Ocean) or to 50°N (Atlantic Ocean), since local sea ice extent and, in particular, its variability through time, may more significantly affect marine reservoir ages at higher latitudes (Heaton *et al.*, 2020b). The Marine20 curve was generated utilising an ocean/atmosphere/biosphere global carbon cycle box model informed by CO₂ data from the polar ice cores and ¹⁴C data from the Northern Hemisphere atmospheric curve (IntCal20).

These revised curves should result in more accurate calibrated ages generated from the radiocarbon dating method. However, it should be noted that “increased accuracy” does not equate to “increased precision”, since the additional, higher frequency structure (“wiggles”) within the updated datasets, which more reliably represent the authentic past variability of atmospheric ¹⁴C concentrations, will lead to broader – or, indeed, multimodal – probability distributions for calibrated ages from certain intervals (e.g., Fig.1). By extension, the increased accuracy of individual calibrated radiocarbon data will lead to increased accuracy (though, again, not necessarily increased precision) of the outputs of (e.g., Bayesian) statistical models that combine these individual data (the “likelihoods”) according to (e.g., stratigraphic) relationships between the samples (the model “prior”).

The three updated radiocarbon calibration curves represent the current best state of knowledge of the international radiocarbon dating community, and are the culmination of decades of work. Nevertheless, on-going research over the coming years and decades will no doubt advance our knowledge yet further, leading to future, ever more robust enhancements of the radiocarbon calibration curves, and improving the ability of the wide ranging ¹⁴C user community to glean robust chronological information in relation to the multitude of scientific areas of investigations dependent upon the technique.

Acknowledgements:

All figures in the present manuscript were made using the Bayesian chronological software OxCal ver.4.4 (<https://c14.arch.ox.ac.uk/oxcal/OxCal.html>), made freely available by Prof. Christopher Bronk Ramsey. On behalf of the global ¹⁴C user community, the authors gratefully thank Prof. Paula Reimer, the outgoing co-ordinator of the “IntCal” (International Calibration) Working Group, for her tireless work in the role over the last two decades. Dr. Ruiliang Liu acknowledges financial support from the European Research Council (ERC) Advanced Grant, “FLAME”, awarded to Prof. A Mark Pollard (Grant No. 670010) and from the University of Oxford John Fell Fund (Grant No. 0007844).

References:

Bronk Ramsey C, Heaton T J, Schlolaut G, Staff R A, Bryant C L, Brauer A, Lamb H F, Marshall M H, Nakagawa T. 2020. Reanalysis of the atmospheric radiocarbon calibration record from Lake Suigetsu, Japan. *Radiocarbon*, 62: doi:10.1017/RDC.2020.18

Chen, F H, Dong G H, Zhang D J, Liu X Y, Jia X, An C B, Ma M M, Xie Y W, Barton L, Ren X Y, Zhao Z J, Wu X H, Jones M K. 2015. Agriculture facilitated permanent human occupation of the Tibetan Plateau after 3600 B.P. *Science*, 347: 248–250

Cheng H, Edwards R L, Southon J R, Matsumoto K, Feinberg J M, Sinha A, Zhou W, Li H, Li X, Xu Y. 2018. Atmospheric $^{14}\text{C}/^{12}\text{C}$ changes during the last glacial period from Hulu Cave. *Science*, 362: 1293–1297

de Vries H L. 1958. Variation in concentration of radiocarbon with time and location on Earth. *Proceedings of the Koninklijke Nederlandse Akademie van Wetenschappen B*, 61: 94–102.

Dong G, Li R, Lu M, Zhang D, James N. 2020. Evolution of human–environmental interactions in China from the Late Paleolithic to the Bronze Age. *Progress in Physical Geography*, 44: 233–250

Heaton T J, Blaauw M, Blackwell P G, Bronk Ramsey C, Reimer P J, Scott E M. 2020a. The IntCal20 approach to radiocarbon calibration curve construction: a new methodology using Bayesian splines and errors-in-variables. *Radiocarbon*, 62: doi:10.1017/RDC.2020.46

Heaton T J, Köhler P, Butzin M, Bard E, Reimer R W, Austin W E N, Bronk Ramsey C, Grootes P M, Hughen K A, Kromer B, Reimer P J, Adkins J F, Burke A, Cook M S, Olsen J, Skinner L C. 2020b. Marine20—the marine radiocarbon age calibration curve (0–55,000 cal BP). *Radiocarbon*, 62: doi:10.1017/RDC.2020.68

Hogg A G, Heaton T J, Hua Q, Palmer J G, Turney C S M, Southon J, Bayliss A, Blackwell P G, Boswijk G, Bronk Ramsey C, Pearson C, Petchey F, Reimer P J, Reimer R W, Wacker L. 2020. SHCal20 Southern Hemisphere calibration, 0–55,000 years cal BP. *Radiocarbon*, 62: doi:10.1017/RDC.2020.59

Libby W F, Anderson E C, Arnold J R. 1949. Age determination by radiocarbon content: world-wide assay of natural radiocarbon. *Science*, 109: 227–228

Miyake F, Nagaya K, Masuda K, Nakamura T. 2012. A signature of cosmic-ray increase in AD 774–775 from tree rings in Japan. *Nature*, 486: 240–242.

Reimer P J, Bard E, Bayliss A, Beck J W, Blackwell P G, Bronk Ramsey C, Brown D M, Buck C E, Edwards R L, Friedrich M. 2013a. Selection and treatment of data for radiocarbon calibration: an update to the International Calibration (IntCal) criteria. *Radiocarbon* 55: 1923–1945

Reimer P J, Bard E, Bayliss A, Beck J W, Blackwell P G, Bronk Ramsey C, Buck CE, Cheng H, Edwards R L, Friedrich M, Grootes P M, Guilderson T P, Haflidason H, Hajdas I, Hatté C, Heaton T J, Hoffmann D L, Hogg A G, Hughen K A, Kaiser K F, Kromer B, Manning S W, Niu M, Reimer R W, Richards D A, Scott E M, Southon J R, Staff R A, Turney C S M, van der Plicht J. 2013b. IntCal13 and Marine13 radiocarbon age calibration curves 0–50,000 years cal BP. *Radiocarbon*, 55: 1869–1887

Reimer P J, Austin W E N, Bard E, Bayliss A, Blackwell P G, Bronk Ramsey C, Butzin M, Cheng H, Edwards R L, Friedrich M, Grootes P M, Guilderson T P, Hajdas I, Heaton T J, Hogg A G, Hughen K A, Kromer B, Manning S W, Muscheler R, Palmer J G, Pearson C, van der Plicht J, Reimer R W, Richards D A, Scott E M, Southon J R, Turney C S M, Wacker L, Adolphi F, Büntgen U, Capano M, Fahrni S M, Fogtmann-Schulz A, Friedrich R, Köhler P, Kudsk S, Miyake F, Olsen J, Reinig F,

Sakamoto M, Sookdeo A, Talamo S. 2020. The IntCal20 Northern Hemisphere radiocarbon age calibration curve (0–55 cal kBP). *Radiocarbon* 62, doi:10.1017/RDC.2020.41

Renfrew C, Liu B. 2018. The emergence of complex society in China: the case of Liangzhu. *Antiquity* 92: 975–990

Accepted Manuscript

Figures:

Figure 1: A comparison of the previous (IntCal13, blue; Reimer *et al.*, 2013b) and recently updated (IntCal20, red; Reimer *et al.*, 2020) radiocarbon calibration curves for the time period 300 BCE to 700 CE, illustrating the impact of the updated calibration curve on a hypothetical sample dating to 1900 ± 25 ^{14}C years Before Present (BP) (grey probability distribution on the y axis). Using IntCal13, highest probability density (HPD) ranges of 78 to 126 cal CE (at 68.3% probability) and 31 to 37, 51 to 171 and 193 to 210 cal CE (95.4% probability) are produced (blue horizontal bars underneath the blue probability density function, PDF); whereas, using IntCal20, HPD ranges of 89 to 91 and 120 to 204 cal CE (at 68.3% probability) and 70 to 215 cal CE (95.4% probability) are produced (red horizontal bars underneath the red PDF). Median ages (plotted as crosses along the PDFs) are 102 cal CE and 150 cal CE, respectively, demonstrating a shift to younger ages of approximately 50 calibrated years using the updated calibrated curve. Both calibration curves are plotted with 1σ uncertainty envelopes.

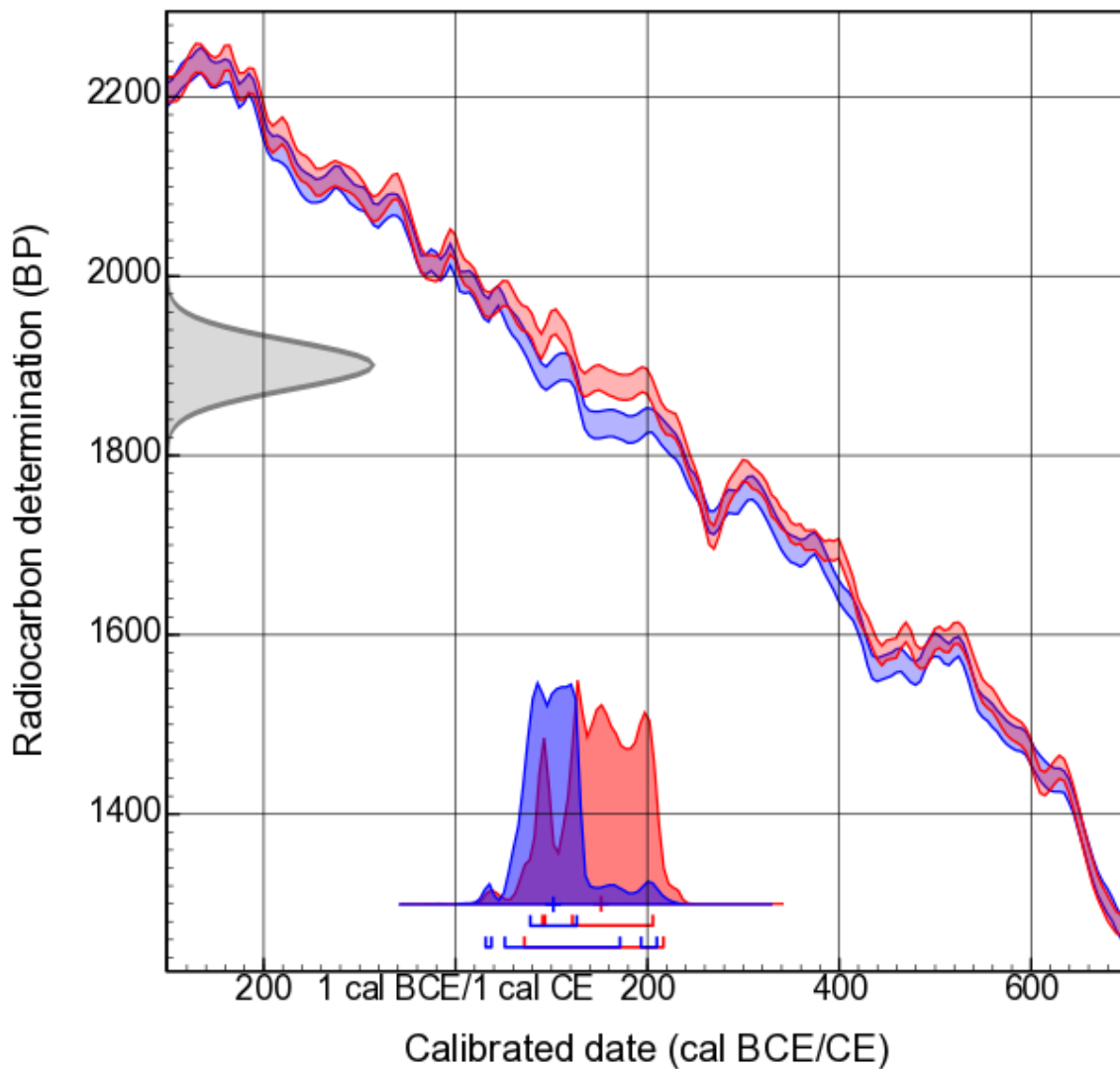


Figure 2: A comparison of the previous (IntCal13, blue; Reimer *et al.*, 2013b) and recently updated (IntCal20, red; Reimer *et al.*, 2020) radiocarbon calibration curves for selected time periods referred to in the main text: (a) 6000 to 2000 cal BP (= 4051 to 51 cal BCE); (b) 10,000 to 6,000 cal BP; (c) 15,000 to 11,000 cal BP; and (d) 50,000 to 30,000 cal BP. Both calibration curves are plotted with 1σ uncertainty envelopes.

